Photochemistry and Photobiology, 1997, 66(6): 872–878

Protein-A–mediated Targeting of Bacteriochlorophyll-IgG to *Staphylococcus aureus*: A Model for Enhanced Site-Specific Photocytotoxicity

Shimon Gross[1,2], Alexander Brandis[2], Louise Chen[1], Varda Rosenbach-Belkin[2], Susanne Roehrs[1,2], Avigdor Scherz[2] and Yoram Salomon*[1]

The Departments of [1]Biological Regulation and [2]Plant Sciences, The Weizmann Institute of Science, Rehovot, Israel

Received 12 June 1997; accepted 12 September 1997

ABSTRACT

A model for studying the efficiency of photodynamic action with a photosensitizer placed exclusively on the bacterial cell wall has been used. Bacteriochlorophyllide molecules, conjugated to rabbit immunoglobulin G (IgG), were synthesized. The conjugated pigment bacteriochlorophyll (Bchl)-IgG bound with high specificity to protein-A residues naturally exposed on the cell wall of the bacterium *Staphylococcus aureus* Cowan I. In bacterial suspensions the phototoxicity of the targeted conjugates (0.5–2.5 pigment per IgG molecule) was dose dependent (LD_{50} = 1.7 μM) in the presence of light ($\lambda > 550$ nm) and inhibited by native IgG but not by ovalbumin, suggesting selective interaction with protein-A on the bacterial cell wall. No dark toxicity was noticed even with the highest conjugate concentration tested. In contrast, the photocytotoxicity of bacteriochlorophyll-serine (Bchl-Ser, LD_{50} = 0.07 μM) used as a nontargeted control was not inhibited by IgG. In spite of its lower apparent potency, Bchl-IgG was found to be 30 times more efficacious than Bchl-Ser: At LD_{50}, only 66 000 Bchl-IgG molecules were bound per bacterium compared to 1 900 000 molecules of Bchl-Ser. The higher efficacy of Bchl-IgG is explained by its exclusive position on the bacterial cell wall. Consequently, photogeneration of oxidative species is confined to the cell wall and its vicinity, a seemingly highly susceptible domain for photodynamic action. In considering the design of cell-specific sensitizers for bacterial and cancer therapies, it would be beneficial to identify the more discretely sensitive subcellular domains as targets.

INTRODUCTION

In photodynamic therapy (PDT)† a photosensitizer, bound to target cells, is illuminated to locally generate cytotoxic singlet oxygen and/or ion radicals (1–6). Although PDT is currently used in tumor therapy, its high potential for bacterial and viral diseases as well as for sterilization purposes has long been recognized (7–11).

In PDT, the requirements for specificity of the carrier system are less stringent than in other drug-targeting modalities (because of the ability to direct the light beam). However, the targeting of photosensitizing molecules to specific cells remains imminent (12–20). Not less important to the efficiency of the photodynamic action is the exact subcellular distribution of the sensitizer.

Herein we set out to explore the efficiency of photodynamic action aimed specifically at the cell surface. Several studies have suggested that membrane-bound sensitizers are highly potent due to their membrane-perforating action and subsequent cell lysis. However, the distribution of photosensitizing molecules in other subcellular compartments rendered the experimental confirmation of this hypothesis difficult. Hence, to test the significance of cell membrane sensitivity in PDT we designed sensitizers that strictly bind to the extracellular wall of gram-positive bacteria and examined their photocytotoxicity. The sensitizer consists of bacteriochlorophyllide a (Bchlide) covalently linked to rabbit polyclonal immunoglobulin G (IgG). The highly specific interaction of IgG with protein-A, a molecule naturally abundant on the outer cell wall of *Staphylococcus aureus* Cowan I, limits the distribution of the sensitizer and confines the photodynamic activity to the outer cellular domain (21,22). The significance of selective membrane distraction by PDT in this bacterial system provides a simple model for examining the advantages of targeted PDT, not only in the case of bacteria, but also when antitumor or antiviral treatments are considered.

The photodynamic activity of the targeted bacteriochlorophyll (Bchl)-IgG conjugate was compared with that of the Bchl-serine (Ser) conjugate, which acts after adherence and simple partition into cells. These conjugates have recently

*To whom correspondence should be addressed at: Department of Biological Regulation, The Weizmann Institute of Science, Rehovot 76100, Israel. Fax: 972-8-934-4116;
e-mail: hsalmon@weizmann.weizmann.ac.il

†*Abbreviations:* Bchl, bacteriochlorophyll; Bchlide, bacteriochlorophyllide; BHI, brain heart infusion; DCC, dicyclohexylcarbodiimide; DMF, dimethylformamide; HPD, hematoporphyrin derivative; IgG, immunoglobulin G; LD_{50}, 50% lethal dose; NHS, *N*-hydroxysuccinimide; OD, optical density; PAGE, polyacrylamide gel electrophoresis; PDT, photodynamic therapy; SDS, sodium dodecyl sulfate; Ser, serine.

been synthesized in our laboratory and found to be highly efficient photodynamic reagents (23–28). The Bchl-Ser is a water-soluble molecule; it has strong absorption at 765–780 nm, it is ~200 times more phototoxic than heamatoporphyrin derivatives (HPD) when tested in cell cultures (50% lethal dose [LD_{50}] = 5×10^{-8} *M*) and clears rapidly from the animal body (16 h) (26). Preliminary results in our laboratory demonstrated that both Bchl-IgG and Bchl-Ser have bactericidal and virucidal effects (29,30).

Here we describe the synthesis and properties of a new, targeted Bchl-IgG conjugate and demonstrate its selective protein-A-mediated binding to the bacterial cell wall and the ensuing superior photodynamic efficiency over the nontargeted Bchl-Ser. This phenomenon is explained by the presumably high susceptibility of the bacterial boundary to the photogenerated cytotoxic oxygen species.

MATERIALS AND METHODS

Materials. Rabbit IgG Cohn fraction V (cat: G-0261) and *N*-hydroxysuccinimide (NHS) were obtained from Sigma Chemical Co. (USA). Europium-labeled rabbit-IgG (Eu-IgG) was kindly provided by Dr. F. Kohen (The Weizmann Institute). Enhancement solution for Eu-delayed fluorescence measurements was from Delfia Turko (Finland). Dicyclohexylocarbodiimide (DCC) was from Pierce (USA) and DEAE-cellulose was from Whatman Chemical Co. (UK). All other chemicals were analytical grade.

Preparation of Bchl derivatives. Bacteriochlorphyll *a* was extracted from lyophilized *Rhodospirillum rubrum* (31); Bchl-Ser and Bchlide were prepared by enzymatic transesterification or hydrolysis of the geranyl-geranyol chain, respectively using chlorophyllase (23,24,32). A 30-fold molar excess of the NHS-activated ester of Bchlide (1.5 mg) dissolved in dimethylformamide (DMF, 200 μL) was added stepwise over 50 min, into a stirring solution containing IgG (11 mg, 2 mL) in carbonate buffer (0.1 *M*, pH 8.6), followed by short sonications. The reaction mixture was stirred for 24 h. All operations were performed under Ar in the dark at 4°C.

Purification of the Bchl-IgG conjugate. The reaction mixture was centrifuged at 15 000 RPM for 10 min and the supernatant dialyzed overnight against 2 × 1000 mL of 10 m*M* Tris-HCl, pH 8.5. The dialyzate was mixed with 5 mL of DEAE-cellulose slurry (50%) that was pre-equilibrated with 10 m*M* Tris-HCl, pH 8.5. The resulting mixture was poured into a small glass column (0.5 cm × 5 cm) and washed with five column volumes of the same buffer. The Bchl-IgG was eluted with 0.5 *M* NaCl in 10 m*M* Tris-HCl, pH 8.5. The 3 mL fractions containing the green Bchl-IgG were pooled and dialyzed overnight at 4°C against 1000 mL of 10 m*M* Tris-HCl, pH 8.5. The product was stored under Ar in the dark at 4°C until further use.

Spectroscopic analysis. Absorption spectra of the purified Bchl-IgG solution were recorded and the concentrations were calculated from the absorption at 770 nm of Bchlide in aqueous solution using $\epsilon = 4.37 \times 10^4$ mol L^{-1} cm^{-1}. This absorption is to some extent solvent dependent and its energy shifts from ~763 to 772 nm (23–25,31,33). The protein concentration of Bchl-IgG was also determined by absorption at 280 nm using $\epsilon = 2.27 \times 10^5$ mol L^{-1} cm^{-1} for IgG. To correct for spectral overlap, protein concentration was calculated as follows: $[IgG] = [OD_{280} - (0.803\ OD_{770})]/2.27 \times 10^5$, where 0.803 is the correction factor relating to the pigment/protein overlap in the Soret band region relative to the pigment's absorption at 770 nm. The Bchl : IgG molar ratios of the various batches of conjugates prepared here were in the range of 0.5–2.5.

The long-wavelength fluorescence of the isolated conjugate (785 nm) corresponds to its lowest energy transition (770 nm). A second fluorescence band, found at ~700 nm probably corresponds to an oxidized form of the conjugate that absorbs at 680 nm and constitutes ~10–15% (in molar ratio) of the final product.

Flame photometry. The concentration of Mg atoms was determined by flame photometry using $MgCl_2$ as a standard (Spectroflame ICP, Germany). The Bchl-Ser was also determined by its Mg content. Results were in good agreement (±10%) with the concentration of Bchl determined by the previously mentioned spectroscopic procedure. We concluded that no significant pheophytinization occurred during conjugation and that the extinction coefficient of the bound Bchl was similar to that of the free pigment.

Sodium dodecyl sulfate polyacrylamide gel electrophoresis (SDS-PAGE). The SDS-PAGE under denaturing conditions was performed as described earlier (34) using 12% SDS and rainbow molecular weight standards (BioRad). Unstained gels were dried and optically scanned.

Light source. All the phototoxicity assays were performed with a home-built xenon lamp with vertical emission providing 140 mW/cm^2 at the target level, using glass or a $Cr_2K_2O_7$ liquid filter transferring light at $\lambda \geq 550$ nm (35).

Bacterial culture. Lyophilized *S. aureus* Cowan I, kindly provided by Prof. Z. Eshar, The Weizmann Institute, were grown in liquid brain heart infusion (BHI) media for 18 h at 37°C with continuous shaking.

Phototoxicity experiments. The standard experimental design consisted of four discrete steps: (1) Preincubation: Fresh bacterial suspensions (200 μL) in 0.1 *M* carbonate buffer, pH 8.6 were incubated with the test sensitizer and/or inhibitor at the indicated concentrations for 1 h in the dark. (2) Wash: Unbound sensitizer was removed by washing and resuspension in the same buffer (3×). (3) Illumination: The bacterial suspensions were exposed to light (140 mW/cm^2, $\lambda > 550$ nm) for 5 min. (4) Assessment of survival: Samples of the bacterial suspensions (30 μL) were cultured in 2 mL of BHI liquid media at 37°C (shaking) for 2 h. Bacterial density was monitored by turbidity measurements at $\lambda = 660$ nm, taking optical density $(OD)_{660} = 1$ for 5×10^7 bacteria/mL. Each experiment consisted of one experimental and three control groups: experimental group: bacteria were subjected to complete treatment (varying one experimental factor); light control: irradiated bacteria, not treated with sensitizer; dark control: nonirradiated bacteria, treated with sensitizer in the dark; untreated control: values used for calculation of 100% survival.

Bchl-IgG binding. The Eu-IgG (36) (120 ng), IgG or Bchl-IgG (0–1 nmol), carbonate buffer, pH 8.6 (10 μmol) and bacteria (5×10^7 prewashed in 0.1 m*M* ovalbumin) were incubated in a final volume of 100 μL for 1 h at 4°C with gentle shaking. The binding reaction was terminated by a 10-fold dilution and by washing (3×) (centrifugation for 2 min, 15 000 RPM) with 1 mL of 0.1 *M* carbonate buffer, pH 8.6 at 4°C. The washed bacterial pellets were then resuspended and incubated for 15 min with enhancement solution (300 μL) at 4°C. The mixtures were then centrifuged at 15 000 RPM in an Eppendorff centrifuge for 5 min to remove the bacteria. Two hundred microliters of the clear supernatant were analyzed for Eu by time-resolved fluorescence using an LKB-Wallac, Arcus 1230 fluorometer. Controls for nonspecific binding contained 0.1 m*M* of free IgG. The values for nonspecific binding were usually less than 1% of the total fluorescence units added and accounted for not more than 10% of the total Eu-IgG bound. Binding was in the range of 10–50% of the total fluorescence units added. Specific binding was calculated by subtracting the values of the nonspecific controls from the total bound values. All values were duplicate determinations. Experiments were conducted at least three times, unless otherwise indicated.

Bchl-Ser uptake. Suspensions of *S. aureus* (10^9 bacteria/20 mL) were incubated with Bchl-Ser (0.05–50 μ*M*) for 1 h at 4°C in 0.1 *M* carbonate buffer, pH 8.6 and later washed with 0.1 *M* Tris-HCl, pH 8.5 to remove any free pigment. The bacterial pellets were resuspended in 1 mL MeOH, sonicated for 1 min and centrifuged. The extracted Bchl-Ser in the supernatant was spectroscopically analyzed (300–850 nm). The concentration of Bchl-Ser was calculated from the absorption assuming $\epsilon^0_{770} = 5.92 \times 10^4$ in MeOH (24). Correction for oxidation products (not more than 10%) absorbing at 680 nm was made assuming $\epsilon^0_{680} = 7.28 \times 10^4$ in MeOH (24).

RESULTS

The spectrum of Bchl-IgG (3 μ*M*) in 0.1 m*M* Tris-HCl, pH 8.5 (Fig. 1a) exhibits four major peaks. Three maxima represent the pigment moiety absorption: the Soret band (360 nm), the Q_x (580 nm) and Q_y (765 nm) transitions and a

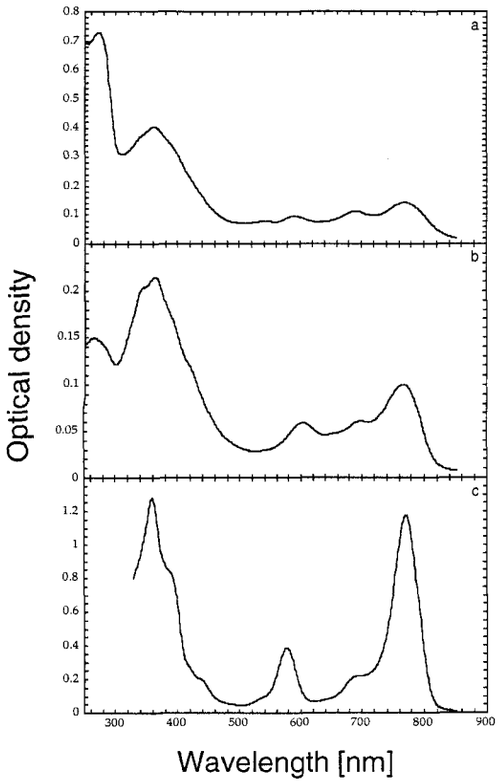

Figure 1. Ultraviolet–visible absorption spectra of Bchl-IgG and Bchl-Ser. The UV–visible absorption spectra of 3 μ*M* Bchl-IgG in 0.1 m*M* Tris-HCl, pH 8.5 (a), 3 μ*M* Bchlide in 0.1 m*M* Tris-HCl, pH 8.5 (b) and of 3 μ*M* Bchlide in acetone (c). The observed spectrum for the current preparation corresponds to 2.0 Bchl per molecule of IgG. Minor shoulders at 430 nm and 680 nm correspond to traces of dark oxidized Bchlide.

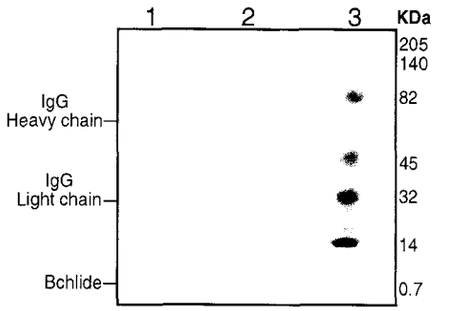

Figure 2. Electrophoretic separation of Bchl-IgG. The SDS-PAGE of Bchlide (lane 1), Bchl-IgG (lane 2) and rainbow molecular weight marker (BioRad, lane 3) was performed using a 12% gel. The gel was not stained. The bands were visually detectable and recorded by a computerized color scanner.

fourth around 280 nm, which is due to the protein absorption. A fifth minor absorption band, at ~680 nm, consists of the 0–1 vibronic component of the Q_y transition and a small contribution from the oxygenated product (see Materials and Methods). The spectra of Bchlide (3 μ*M*) in 0.1 m*M* Tris-HCl, pH 8.5 (Fig. 1b) and in acetone (Fig. 1c) represent the unbound pigment.

The Bchl-IgG conjugation was verified by SDS-PAGE (Fig. 2). Visual examination of the unstained gel revealed two blue-green-colored bands at ~62 kDa and ~28 kDa, representing the Bchl conjugates of the heavy and light chains of IgG, respectively (lane 2). The protein content of these bands was also confirmed by Coomassie brilliant blue staining of the same gel. The green band of Bchlide at the lower molecular weight region was also visible (lane 1). These results indicated that the Bchl-IgG preparation was free of unbound pigment and covalent protein–protein conjugates.

The photocytotoxicities of Bchl-IgG and Bchl-Ser depend both upon the sensitizer concentration and light (Fig. 3). The corresponding LD_{50} values were 1.7 ± 0.3 and 0.07 ± 0.02 μ*M* SEM, respectively (n = 3). Note that up to the highest tested sensitizer concentration (10 μ*M*), Bchl-IgG and Bchl-Ser had no detectable dark toxicity.

To examine whether Bchl-IgG confers phototoxicity by binding to protein-A residues or to arbitrary sites on the targeted bacteria, we tested the competition of the phototoxic effect by adding natural IgG (Fig. 4). It can be seen that the addition of 0.1 m*M* IgG almost totally abolished the phototoxic damage induced by Bchl-IgG. However, IgG, as expected, had no effect on the phototoxicity of the nontargeted Bchl-Ser (Table 1). Ovalbumin, at the same concentration, caused only a small and insignificant inhibition of the phototoxic effect induced by Bchl-IgG, which seemed not to be competitive. Cumulatively, these results suggest that Bchl-IgG confers phototoxicity to *S. aureus* only by binding to protein-A residues. In order to quantitate the phototoxic effects of Bchl derivatives, we determined the number of protein-A binding sites on these bacteria. The binding of rabbit-IgG was determined using Eu-IgG (Fig. 5A). Scatchard analysis (Fig. 5A, insert) revealed that B_{max} = 220 ± 50 fmol/

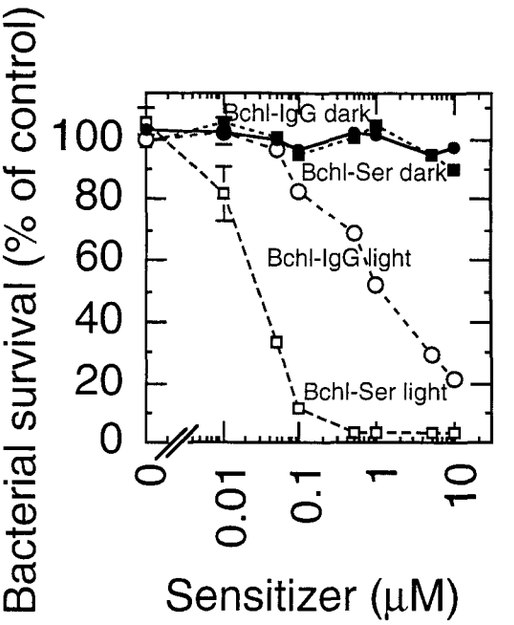

Figure 3. Dose-dependent phototoxicity of Bchl-IgG and Bchl-Ser on *S. aureus*. Bacteria and photosensitizer at the indicated concentrations were incubated for 60 min. Irradiation at 140 mW/cm² was for 5 min (λ > 550 nm). All other details were as described in the Materials and Methods section.

10^6 bacteria SEM (n = 3), *i.e* 132 000 ± 30 000 IgG binding sites per bacterium. The dissociation constant (K_d) for IgG binding was calculated to be 1.3 ± 0.7 μ*M* SEM (n = 3).

The binding of Bchl-IgG to the bacteria was determined in a competition study with Eu-IgG (Fig. 5A). The K_d and B_{max} values of Bchl-IgG (2.7 ± 1.0 μ*M* SEM and 210 fmol/10^6 bacteria, respectively) were very similar to those of Eu-IgG, indicating that the binding properties of the protein were not impaired by the conjugation procedure. The phototoxicities of Bchl-IgG ($LD_{50[Bchl\text{-}IgG]}$ = 1.7 ± 0.3 SEM [Fig. 3]) and ($K_{d[Bchl\text{-}IgG]}$ = 1.3 ± 0.7 SEM [Fig. 5A]), respectively, were about the same, suggesting that binding of Bchl-IgG to the bacteria is the rate-limiting step in the toxic effect.

The adsorption of Bchl-Ser to *S. aureus* was found to correlate the phototoxic activity of Bchl-Ser to the amount of bound pigment (Fig. 5B). Up to 10 μ*M* (the highest concentration tested), the adsorption of Bchl-Ser to the bacteria appeared linear, with concentrations reaching a value of 7.8 × 10^6 molecules/bacterium (Fig. 5B). In comparison, the phototoxicity of Bchl-Ser in the same concentration range was sigmoidal, with an LD_{50} at 0.07 μ*M* Bchl-Ser or 1.9 × 10^6 Bchl-Ser molecules/bacterium. Maximal phototoxicity was observed at 0.5 μ*M* (2.1 × 10^6 molecules/bacterium) above which no further increase was observed.

In spite of applying the same light dose, a 20-fold difference in LD_{50} between the two photosensitizers was observed (Fig. 3). Interestingly, we calculated that at the respective LD_{50} values, only 66 000 molecules of Bchl-IgG were needed, compared to 1 900 000 molecules/bacterium of Bchl-Ser. This result suggested a ~29-fold higher phototoxic efficiency of Bchl-IgG.

The efficiency of the photolytic process was calculated by determining the minimal number of photons required to kill a single bacterium after treatment with either Bchl-IgG or Bchl-Ser at LD_{50}. The calculation was performed as follows: The light intensity (I) at the target level was

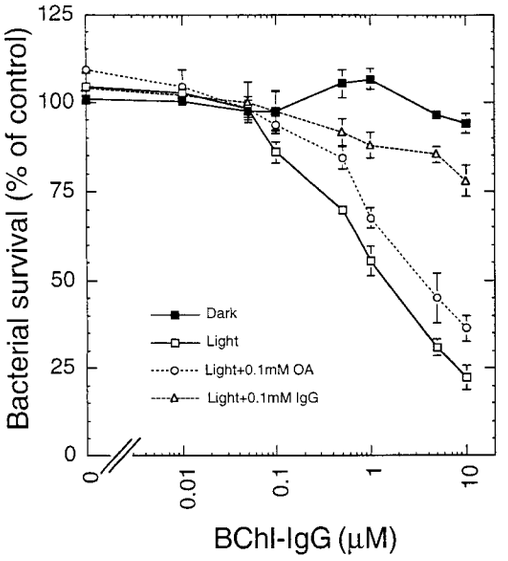

Figure 4. Site-specific photolysis of *S. aureus* by Bchl-IgG: Photolysis of *S. aureus* suspensions treated with the indicated concentrations of Bchl-IgG in the absence or presence of 0.1 m*M* IgG or 0.1 m*M* ovalbumin. All other conditions were the same as in Fig. 3.

$$I = 1000\ \mu E\ cm^{-2}\ (300\ s,\ \lambda > 550\ nm). \quad (1)$$

The overall number of photons emitted, nP(T), is given by

$$nP(T) = N_A I\tau = 1.8 \times 10^{23}\ photons\ cm^{-1} \quad (2)$$

where N_A is Avogadro's number and τ is the irradiation time in seconds.

The cross section for Bchl absorption, σ, is given by

$$\sigma = 2303\epsilon' N_A^{-1} = 1.9 \times 10^{-14}\ cm^2\ Bchl^{-1} \quad (3)$$

where ε′ is the integrated absorption of the sensitizer at the provided illumination range (> 550 nm).

With Bchl-IgG, at LD_{50} (1.7 μ*M* Bchl-IgG) approximately 33 000 Bchl-IgG molecules were bound per bacterium (equivalent to 66 000 pigment molecules bound per bacterium) occupying ~25% of the protein-A sites (see Fig. 5). The total available cross section for absorption/bacterium, σT, is given by

$$\sigma T = nB\sigma = 1.25 \times 10^{-9}\ cm^2. \quad (4)$$

The cross-section area of a single bacterium, S_b, is given by

$$S_b = \pi R^2 = 2.2 \times 10^{-8}\ cm^2\ bacterium^{-1}, \quad (5)$$

where R is the approximate radius of the bacterium (1.5 μm). The probability, P_1, of a single photon to be absorbed by a Bchl molecule, given that this photon has reached the bacterium is given by

$$P_1 = \sigma T S_b^{-1} = 0.055\ or\ 5.5\%. \quad (6)$$

The probability, P_2, of a single photon to hit a single bacterium is given by

$$P_2 = V_{bac}\ D_{bac}^{-1} = 0.01\ or\ 1\% \quad (7)$$

where V_{bac} is the volume of a single bacterium ($4\pi R^3/3\ cm^{-3}$ $bacterium^{-1}$) and D_{bac} is the density of the bacterial suspension (2.5 × 10^8 bacteria cm^{-3}).

The total probability, P_3, for photon absorption by Bchl is therefore given by

$$P_3 = P_1 \times P_2 = 5.5 \times 10^{-4}\ or\ 0.055\%. \quad (8)$$

The total number of photons absorbed by Bchl molecules in 1 mL of bacterial suspension, nP(A), during 5 min of illumination is given by

$$nP(A) = nP(T) \times P_3 = 1 \times 10^{20}\ photons. \quad (9)$$

Therefore the minimal number of photons required to kill a single bacterium nP(B) at LD_{50} is given by

$$nP(B) = nP(A)D_{bac}^{-1} = 4 \times 10^{11}\ photons/bacterium. \quad (10)$$

With Bchl-Ser, at LD_{50} (0.07 μ*M*), the number of Bchl-Ser molecules bound/bacterium is given by

$$nB = 1.9 \times 10^6\ Bchl\text{-}Ser/bacterium. \quad (11)$$

Therefore at the same light dose: $\sigma T = nB\sigma = 3.4 \times 10^{-8}$ cm^2. P_1 = 1.6 or 160%, $P_3 = 1.6 \times 10^{-2}$ or ~1.6% and nP(A) = 2.9 × 10^{21} photons. Hence

$$nP(B) = 1.16 \times 10^{13}\ photons/bacterium. \quad (12)$$

To express the added photolytic efficiency of the sensitizer achieved by targeting, we defined (Δτ) as the reciprocal ratio between the respective intrinsic photolytic efficiencies of the targeted and nontargeted sensitizers

Table 1. The photocytotoxicity and the photolytic efficiency of Bchl-Ser and Bchl-IgG on *S. aureus*

	Phototoxicity (LD_{50}) (μM)			Photoefficiency	
	−	+ IgG (0.1 mM)	+ OA (0.1 mM)	nB* (10^6 molecules/ bacterium)	nP(B)† (10^{10} photons/ bacterium)
Bchl-Ser	0.07 ± 0.02 (n = 3)	0.08	—	1.9	1160
Bchl-IgG	1.7 ± 0.3 (n = 3)	>10	2.5 ± 0.4 (n = 3)	0.066	40

*nB = no. of sensitizer molecules bound to a single bacterium at LD_{50}.
†nP(B) = no. of photons required to kill a single bacterium at LD_{50}.

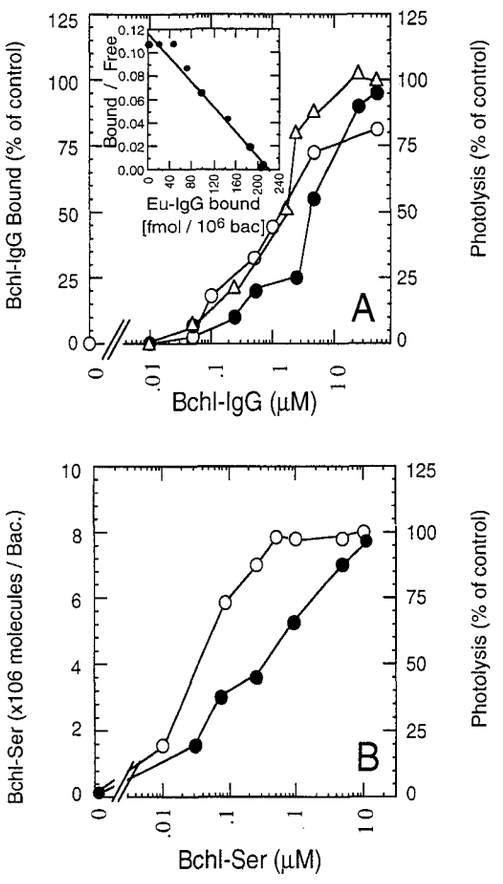

Figure 5. Binding and phototoxicity of Bchl conjugates. (A) Bchl-IgG: The *S. aureus* suspensions were incubated with increasing concentrations of IgG or Bchl-IgG and a constant concentration of Eu-IgG. After incubation (1 h, 4°C), the bacteria were washed and the amount of bound Eu-IgG was measured. The bacterial-bound IgG (△) and Bchl-IgG (●) concentrations were determined and plotted. Phototoxicity data (○) were inserted from Fig. 3. The inserted plot represents Scatchard analysis of the Bchl-IgG binding data. The calculated K_d and B_{max} were 1.3 μM and 220 fmol/10^6 bacteria (132 000 binding sites/ bacteria) respectively. (B) Bchl-Ser: The *S. aureus* suspensions were incubated with increasing concentrations of Bchl-Ser. After incubation (1 h, 4°C) the bacteria were washed, the bacterial-bound Bchl-Ser was extracted with MeOH and the Bchl-Ser concentration determined spectroscopically and plotted against Bchl-Ser concentration (●). Phototoxicity data (○) were inserted from Fig. 3. All other details were as described in the Materials and Methods section.

$$\Delta\tau = nP(B)_{Bchl\text{-}Ser}/nP(B)_{Bchl\text{-}IgG} \quad (13)$$

for Bchl-IgG compared to Bchl-Ser to be

$$\Delta\tau \text{ (Bchl-IgG)} = 29,$$

which is a value expressing the benefit of targeting in this particular system.

DISCUSSION

The efficiency of cellular intoxication by PDT depends upon the distribution of the photosensitizer, in particular, subcellular domains and its state of aggregation. Several studies have indicated cell membranes as preferred targets for PDT but the significance of membrane perforation could not be fully examined due to the presence of sensitizers in other subcellular sites. Here we have used a simple model to test the contribution of photosensitization initiated at a well-defined location: the extracellular cell wall of a bacterium. The model relies on the binding of Bchl-IgG to protein-A molecules exclusively located on the cell wall of *S. aureus* (21,22). Illumination of the bound pigments intoxicates the bacteria with very high quantum yield.

The spectral, biochemical and photocytotoxic properties of the newly synthesized Bchl-IgG conjugate were examined. The results suggested that the chemical manipulations involved in the synthesis of the conjugate have not altered the spectral properties of the pigment (Fig. 1) or the protein-A binding parameters of IgG (Fig. 5). The optimal molar ratio for successful conjugation was found to be 30:1 Bchlide-NHS per IgG, yielding 0.5–2.5 Bchl per IgG with a yield of ~10% by pigment, permitting a final working concentration of 5–20 μM.

The Bchl-Ser and Bchl-IgG were found to be highly phototoxic to *S. aureus*. This was expected because gram-positive bacteria are highly susceptible to PDT, whereas gram-negative strains are less (8,37,38). Although the phototoxicity of both preparations was based on the same chromophore, the phototoxicity of the Bchl moiety in the antibody-conjugated form was 29 times higher than that of Bchl-Ser. Only about 66 000 molecules of Bchl-IgG compared to approximately 1 900 000 molecules of Bchl-Ser were needed for cell intoxication. Yet the LD_{50} of the latter was much lower (0.07 μM for Bchl-Ser compared to 1.7 μM for Bchl-IgG) (Fig. 3 and Table 1). This observation may be related to the different uptake mechanisms and the intrabacterial distributions involved. The phototoxicity of Bchl-IgG was in-

hibited by excess free IgG, and that of Bchl-Ser was not, suggesting specific binding of the former to the bacteria *via* protein A. The Bchl-Ser appears to adsorb/partition into the bacteria in a nonspecific manner (Table 1).

The similarity of the LD_{50} and K_d values for Bchl-IgG (1.7 ± 0.3 and 2.7 ± 0.7 μM SEM [n = 3], respectively) is in agreement with the assumption that sensitizer binding is the rate-limiting step of the photolytic process.

The location of protein-A on the bacterial cell wall confines the bound Bchl-IgG exclusively to that same domain located immediately external to the cell membrane. The higher intrinsic photolytic efficiency of Bchl-IgG compared to the nontargeted Bchl-Ser may be explained as follows: (1) The restricted subcellular localization of Bchl-IgG on the cell wall selectively exposes this organelle and possibly the adjacent cytoplasmic membrane to the highest rate of damage. Our results suggest that the reactive photoproducts generated by sensitization of the externally located pigment molecules are likely to damage the cell wall. Damage to the cell membrane, however, would appear much more critical because spheroplasts from which the cell wall was artificially removed are known to be fully viable. The role of these two cellular domains in conferring susceptibility to PDT agents in gram-positive bacteria, as well as their special orientation have been extensively discussed by Malik and co-workers (8). (2) The high density of the adsorbed Bchl-Ser may result in an internal filter effect, thereby reducing the photochemical efficiency of the process and may enhance self destruction by photobleaching. Using this logic, the major photodamage induced by Bchl-Ser may occur in regions that are less critical to the viability of the organism. This result therefore suggests that the exclusive attachment of fewer sensitizer molecules to a critical subcellular domain may create intensive local photodamage with higher efficiency. The association of Bchl-IgG with any subdomains of a bacterium other than protein-A was ruled out by the finding that the binding and phototoxicity of this sensitizer were totally inhibited by IgG. The added dividend of the targeted photolytic efficiency of the sensitizer $\Delta\tau$ therefore takes into account its subcellular distribution on the one hand and the susceptibility and vital role of the damaged organelle and their special coincidence as well as possible spectral interactions like self absorbency on the other.

The selective and light-dependent destruction of human T leukemia cells by chlorin e_6 conjugated to anti-T cell monoclonal antibodies (ratio = 30:1 PS/Ab) has been described by Oseroff *et al.* (13). The minimal number of photons that were required to kill a single T cell was calculated to be [$nP(B) = 5 \times 10^{10}$ photons/cell]. However, these findings cannot be compared to ours because they calculated the available cross section for absorption of chlorin e_6 (σ) by using the molar extinction (ϵ), suitable for using monochromatic light, while in practice, they used broad-wavelength light (630–670 nm). Their numbers therefore must be larger than reported.

Because of the binary nature of photodynamic biodestruction (drug and light), the targeting of photosensitizers presents a significant advantage compared to other targeted reagents in clinical use. Here the phototoxic activity of the drug can be precisely controlled in space and time (18), *i.e.* that unwanted toxic side effects during the delivery phase, prior to drug accumulation in the target site, can be avoided by precise timing and accurate positioning of the sensitizing light beam. However, the internalization of PDT reagents at sufficiently high concentrations is difficult to achieve. Therefore, induction of cell toxicity on the extracellular surface, as shown here, is of high significance. This is true for PDT applications where treatment of pathogenic microorganisms (viruses, bacteria or fungi) is attempted with confined infections (20) or in PDT of malignant tumors (12–19). In this context, Bchl conjugates, in particular, have the great spectral advantage (λ_{max} = 780 nm), allowing for enhanced penetration depth of the exiting light beam.

Acknowledgements—Y.S. is the incumbent of the Charles and Tillie Lubin Chair of Biochemical Endocrinology. This study was performed in partial fulfillment of S.G.'s M.Sc. thesis for the Feinberg Graduate School, the Weizmann Institute of Science. We thank Dr. Vlad Brumfeld, Dr. Fortüne Kohen and Mr. Dror Noy for their skillful help and Ms. R. Benjamin for her secretarial assistance. This study was supported in part by grants from the Lynne and William Frankel Fund for the Diagnosis and Treatment of Ovarian and Breast Cancer, the Jaffe Family Foundation, Mrs. S. Zuckerman, Yeda Research and Development Co. Ltd. (Israel), the Israeli Ministry of Science and Technology, the Commission of the European Communities and STEBA BEHEER N.V.

REFERENCES

1. Foote, C. S. (1990) Chemical mechanisms of photodynamic action. *Proc. SPIE Inst.* **6**, 115–126.
2. Pass, H. V. (1993) Photodynamic therapy in oncology: mechanisms and clinical use. *J. Natl. Cancer Inst.* **85**, 443–456.
3. Dougherty, T. J. (1993) Photodynamic therapy. *Photochem. Photobiol.* **58**, 895–900.
4. Henderson, B. W. and T. J. Dougherty (1992) How does photodynamic therapy work? *Photochem. Photobiol.* **55**, 145–157.
5. Weishaupt, K. R., C. J. Gomer and T. J. Dougherty (1976) Identification of singlet oxygen as the cytotoxic agent in photoinactivation of a murine tumor. *Cancer. Res.* **36**, 2326–2329.
6. Das, M., H. Mukhtar, E. R. Greenspan and D. R. Bickers (1985) Photoenhancement of lipid peroxidation associated with the generation of reactive oxygen species in hepatic microsomes of hematoporphyrin derivative-treated rats. *Cancer Res.* **45**, 6328–6330.
7. Venezio, F. R., R. DiVincenzo, R. Sherman, T. C. Reichman, K. Origitano, K. Tomphson and O. H. Reichman (1985) Bactericidal effects of photoradiation therapy with hematoporphyrin derivative. *J. Infect. Dis.* **151**, 166–169.
8. Malik, Z., J. Hanania and Y. Nitzan (1990) Bactericidal effects of photoactivated porphyrins; an alternative approach to antimicrobial drugs. *J. Photochem. Photobiol. B: Biology* **5**, 281–293.
9. Nitzan, Y., R. Dror, H. Ladan, Z. Malik, S. Kimel and V. Gottfried (1995) Structure–activity relationship of porphines for photoinactivation of bacteria. *Photochem. Photobiol.* **62**, 342–347.
10. Millson, C. E., M. Wilson, A. J. MacRobert and S. G. Bown (1996) Ex-vivo treatment of gastric *Helicobacter* infection by photodynamic therapy. *J. Photochem. Photobiol. B: Biology* **32**, 59–65.
11. Ben-Hur, E. and B. Horowiz (1995) Advances in photochemical approaches for blood sterilization. *Photochem. Photobiol.* **62**, 383–388.
12. Mew, D., C.-K. Wat, G. H. N. Towers and J. G. Levy (1983) Photoimmunotherapy: treatment of animal tumors with tumor-specific monoclonal antibody–hematoporphyrin conjugates. *J. Immunol.* **130**, 1473–1477.
13. Oseroff, A. R., D. Ohuoha, T. Hasan, J. C. Bommer and M. L. Yarmush (1987) Antibody-targeted photolysis: selective photodestruction of human T-cell leukemia cells using monoclonal antibody–chlorin e_6 conjugates. *Proc. Natl. Acad. Sci. USA* **83**, 8744–8748.

14. Steele, K. J., D. Liu, N. Davis and H. Deal (1989) The preparation and application of porphyrin-monoclonal antibodies for cancer therapy. *Proc. SPIE* **1065**, 73–79.
15. Li, D. and B. D. Zhong (1990) Experimental study of anti-tumor effects with conjugate of monoclonal antibody and hematoporphyrin derivative. *Third biennial meeting of the International Photodynamic Association,* Buffalo, NY.
16. Friedberg, J. S., R. G. Tompkins, S. L. Rakestraw, S. W. Warren, A. J. Fischman and M. L. Yarmush (1991) Antibody-targeted photolysis. Bacteriocidal effects of Sn (IV) chlorin e6–dextran–monoclonal antibody conjugates. *Ann. N.Y. Acad. Sci.* **618**, 383–393.
17. Ming-Lu, X., E. Stevens, T. Lee, L. Strong and A. J. Fischman (1992) Sn-chlorin e6 antibacterial immunoconjugates. *J. Immunol. Methods* **156**, 85–99.
18. Hasan, T. (1992) Photosensitizer delivery mediated by macromolecular carrier systems. In *Photodynamic Therapy, Basic Principles and Clinical Applications* (Edited by B. W. Henderson and T. J. D. Dougherty), pp. 187–200. Marcel Dekker, New York.
19. Schmidt, S. (1993) Antibody-targeted photodynamic therapy. *Hybridoma* **12**, 539–541.
20. Berthiaume, F., S. R. Reiken, M. Toner, R. G. Tompkins and M. L. Yarmush (1994) Antibody-targeted photolysis of bacteria in-vivo. *Biotechnology* **12**, 703–706.
21. Forsgren, A. and J. Sjoquist (1966) Protein A from *Staphylococcus aureus.* I. Pseudo-immune reaction with human γ-globulin. *J. Immunol.* **97**, 822–827.
22. Kronvall, G., P. G. Quie and R. J. Williams (1970) Quantitation of staphylococcal protein A: determination of equilibrium constant and number of protein A residues on bacteria. *J. Immunol.* **104**, 273–278.
23. Scherz, A., Y. Salomon and L. Fiedor (1994) Chlorophyll and bacteriochlorophyll derivatives, preparation and pharmaceutical compositions comprising them as photosensitizers for photodynamic therapy. *Chem. Abst.* **120**, 386.
24. Scherz, A., Y. Salomon and L. Fiedor (1997) Chlorophyll and bacteriochlorophyll derivatives, their preparation and pharmacological compositions comprising them. US Patent No. 5,650,292.
25. Fiedor, L. (1994) Modified chlorophylls as models for primary photosynthesis and photosensitizers for photodynamic therapy of cancer. Ph.D. thesis, The Weizmann Institute of Science, Rehovot, Israel.
26. Rosenbach-Belkin, V., L. Chen, L. Fiedor, I. Tregub, F. Pavlotsky, V. Brumfeld, Y. Salomon and A. Scherz (1996) Serine conjugates of chlorophyll and bacteriochlorophyll: phototoxicity *in vitro* and tissue distribution in mice bearing melanoma tumors. *Photochem. Photobiol.* **64**, 174–181.
27. Fiedor, L., V. Rosenbach-Belkin, M. Sai and A. Scherz (1996) Preparation of tetrapyrole-amino acid covalent complexes. *Plant Physiol. Biochem.* **34**, 393–398.
28. Zilberstein, J., A. Bromberg, A. Franz, V. Rosenbach-Belkin, A. Kritzmann, R. Pefferman, A. Scherz and Y. Salomon (1997) Light dependent oxygen consumption in bacteriochlorophyll-serine treated melanoma tumors: on-line determination using a tissue-inserted oxygen microsensor. *Photochem Photobiol.* **65**, 1012–1019.
29. Chen, L., V. Rosenbach-Belkin, V. Brumfeld, Y. Salomon and A. Scherz (1996) Photodynamic inactivation of bacteria by chlorophyll-serine. The World Association for Laser Therapy (WALT), Jerusalem, Israel.
30. Gross, S., A. Brandis, L. Chen, S. Roehrs, A. Scherz and Y. Salomon (1997) Targeted bacteriochlorophyll: a novel selective photosensitizer for PDT. *Acta Bio-Opt. Informat. Med.* **3**, 21.
31. Rosenbach-Belkin, V. (1988) The primary reactants in bacterial photosynthesis modeling by in vitro preparation. Ph.D. thesis, The Weizmann Institute of Science, Rehovot, Israel.
32. Shapira, A., E. E. Goldschmidt and A. Altman (1987) Chlorophyll catabolism in senescing plant tissues: *in-vivo* breakdown intermediates suggest different degradative pathway for citrus fruit and parsley leaves. *Proc. Natl. Acad. Sci. USA* **84**, 1901–1905.
33. Scherz, A. and V. Rosenbach-Belkin (1989) Comparative study of optical absorption and circular dichroism of bacteriochlorophyll oligomers in Triton X-100, the antenna pigment B850, and the primary donor P-860 of photosynthetic bacteria indicates that all are similar dimers of bacteriochlorophyll a. *Proc. Natl. Acad. Sci. USA* **86**, 1505–1509.
34. Shafir, I., J. Schmidt-Sole, E. Shai and Y. Salomon (1993) The melanocyte-stimulating hormone (MSH) receptor in M2R mouse melanoma tumors: solubilization and properties of the receptor–MSH complex and its covalently crosslinked conjugate. *Melanoma Res.* **3**, 157–168.
35. Parker, C. A. (1968) Photoluminescence of solutions with applications to photochemistry and analytical chemistry. Elsevier, Amsterdam.
36. Lovgren, T., I. Hemmila, K. Pettersson and P. Halonen (1985) Time resolved fluorometry in immunoassays. In *Alternative Immunoassays* (Edited by W. P. Collins), pp. 203–217. Wiley, New York.
37. Malik, Z., H. Ladan and Y. Nitzan (1992) Photodynamic inactivation of gram-negative bacteria: problems and possible solutions. *J. Photochem. Photobiol. B: Biology* **14**, 262–266.
38. Minnock, A., D. I. Vernon, J. Schofield, J. Griffiths, J. H. Parish and S. T. Brown (1996) Photoinactivation of bacteria. Use of a cationic water-soluble zinc phthalocyanine to photoinactivate both gram-negative and gram-positive bacteria. *J. Photochem. Photobiol. B: Biology* **32**, 159–164.